Supporting information for

Single-Material Solvent-Sensitive Actuator from Poly(ionic liquid) Inverse Opals based on Gradient Dewetting

Hua Wu[a]†, Minxuan Kuang[b]†, Liying Cui[a]†, Di Tian[b], Minghui Wang[a], Guoyou Luan*[,a], Jingxia Wang*[,b] and Lei Jiang[b]

1. Experiment

1.1 Fabrication of photonic crystal (PC) template

The glass slides were cut to 3×2 cm and plasma treated to be superhydrophilic. The PC template was obtained by immersing the glass slide into the Ply(St-MMA-AA) latex suspension with 0.5 wt% by vertical deposition at 60℃, 60% RH for abou 24 h.

1.2 Preparation of ionic liquid prepolymer

0.6 g1-vinyl-3-ethylimidazolium bromide (VEA, Lanzhou Greenchem ILs, LICP, CAS), 0.2 g methylmethacrylate (MAA, J&k), 0.5 g methylene-bis-acrylamide (Sigma-Aldrich) and 10 μl 2,2-diethoxyacetophenone (photoinitiator, J&K) were added into 3 ml anhydrous methanol and stirred for 10 min under the protection of N_2. Wherein, the amount of the VEA varies from 0~0.8 g accompanied with varying MAA from 0.8~0 g (the total amount of VEA and MMA is 0.8 g).

1.3 Fabrication of PIL inverse opals

The ionic liquid prepolymer was carefully dropped into the interstice of PC template and then covered by a glass slide. After the ionic liquid prepolymer was photopolymerized under UV light for 2 hours, the sample was immersed into tetrahydrofuran to remove the PC template.

2. Characterization

The as-prepared PIL inverse opal was cut into rectangles with the dimension of 2 cm *0.5 cm and then put on a clean glass slide. Different solvents were dropped on the PIL inverse opal. Excessed solvent was removed by filter paper. Side-view camera was employed to record the actuating process. The structures of PIL inverse opals were characterized by SEM (S-4800, Japan Hitachi) operating at 5.0 kV. UV-vis spectra were collected using a Hitachi U-4100. The contact angles were measured on an OCA20 machine (DataPhysics, Germany) at ambient temperature. FTIR spectrum was recorded on an infrared spectrometer (Bruker, VERTEX 70, 36×, NA = 0.5).

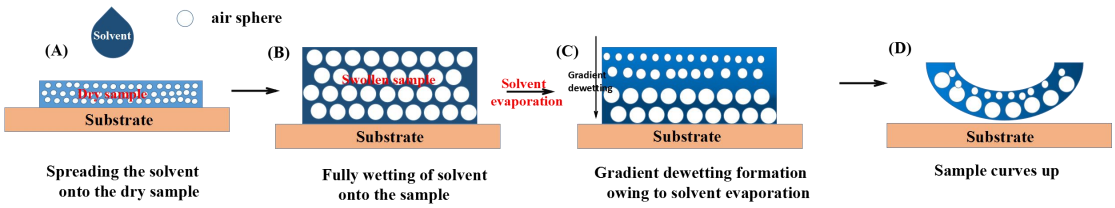

Figure S1. Scheme illustration for the actuator process of the single-material solvent-sensitive actuator

The actuator formation process can be explained as Figure S1: Firstly, dropping the solvent onto the as-prepared Poly ionic liquid inverse opal (A), and then the sample was fully swollen by the solvent in (B). Subsequently, the gradient dewetting forms owing to the solvent evaporation, producing the shrinkable, partly-shrinkable and non-shrinkable region (C) from upper to lower part. These non-inhomogeneous shrinkage results in the actuator formation, the sample curves up (D).

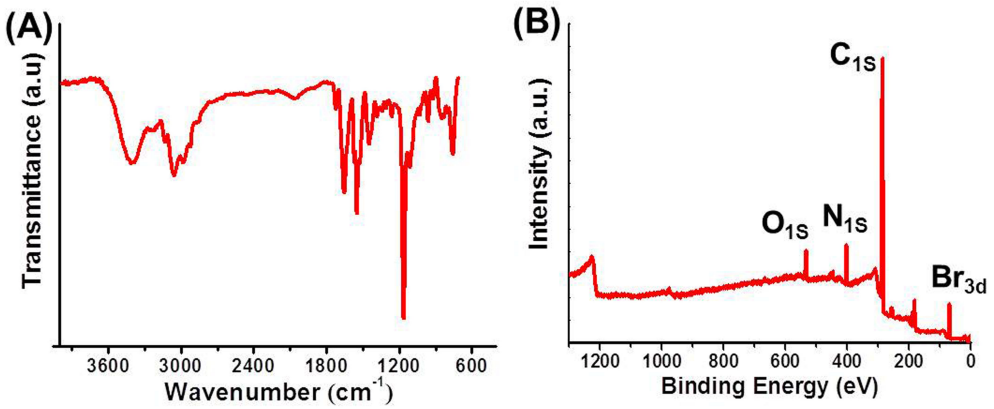

Figure S2. Characterization of the as-prepared poly(ionic liquid) inverse opals. (A) FTIR spectra and (B) XPS result.

Figure S2 presents the FTIR spectra with characteristic peak of 1657, 1550, 1450, 1164 cm^{-1}, which correspond to the vibration of imidazole ring. The FTIR spectra gave a clear characterization of its unique chemical structure of PIL. The element characterization of the XPS suggests the chemical composition of the inverse opals, confirming the formation of PIL inverse opals.

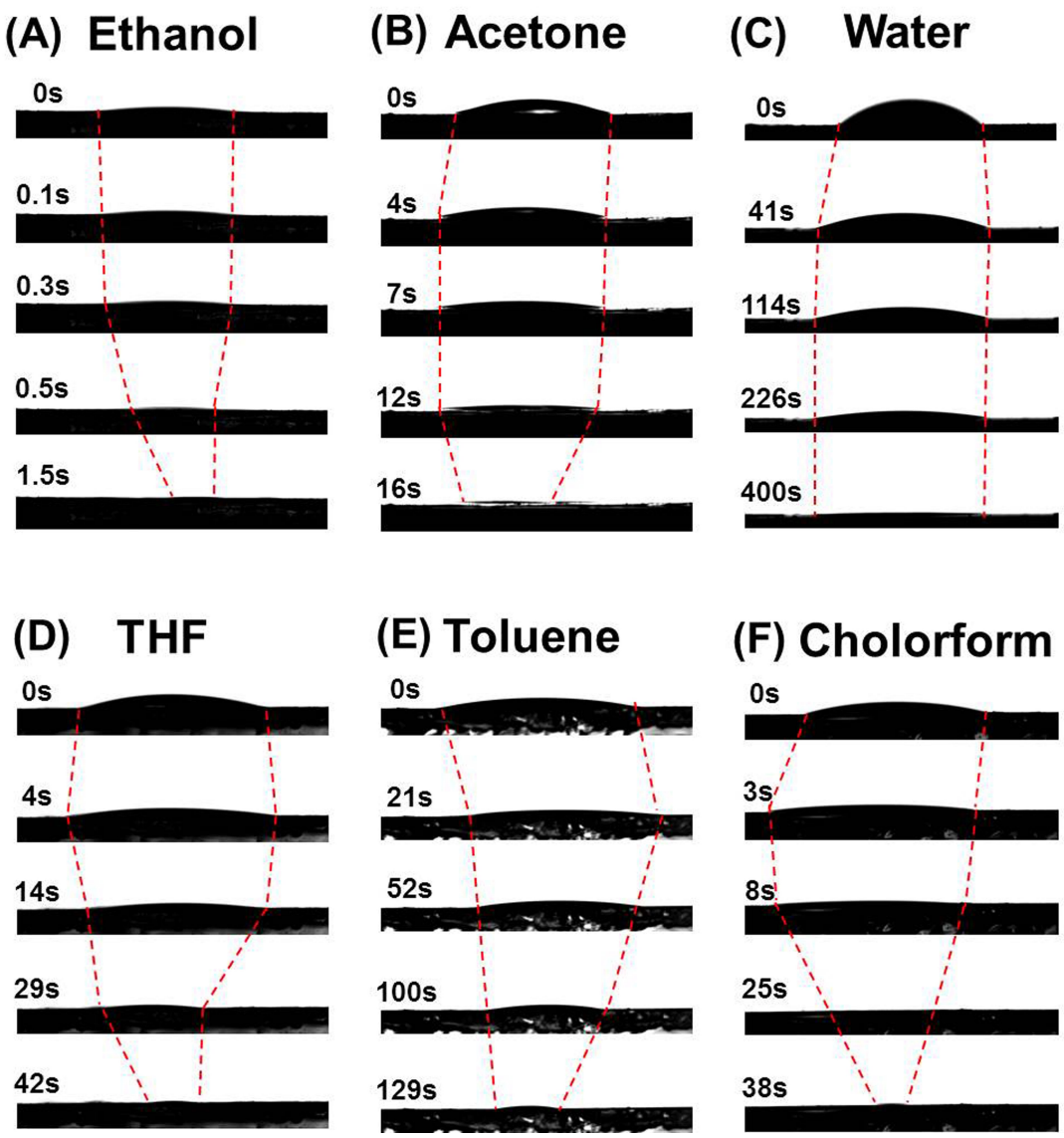

Figure S3. The side-view morphology of varied solvent droplets on PIL films during evaporation process.

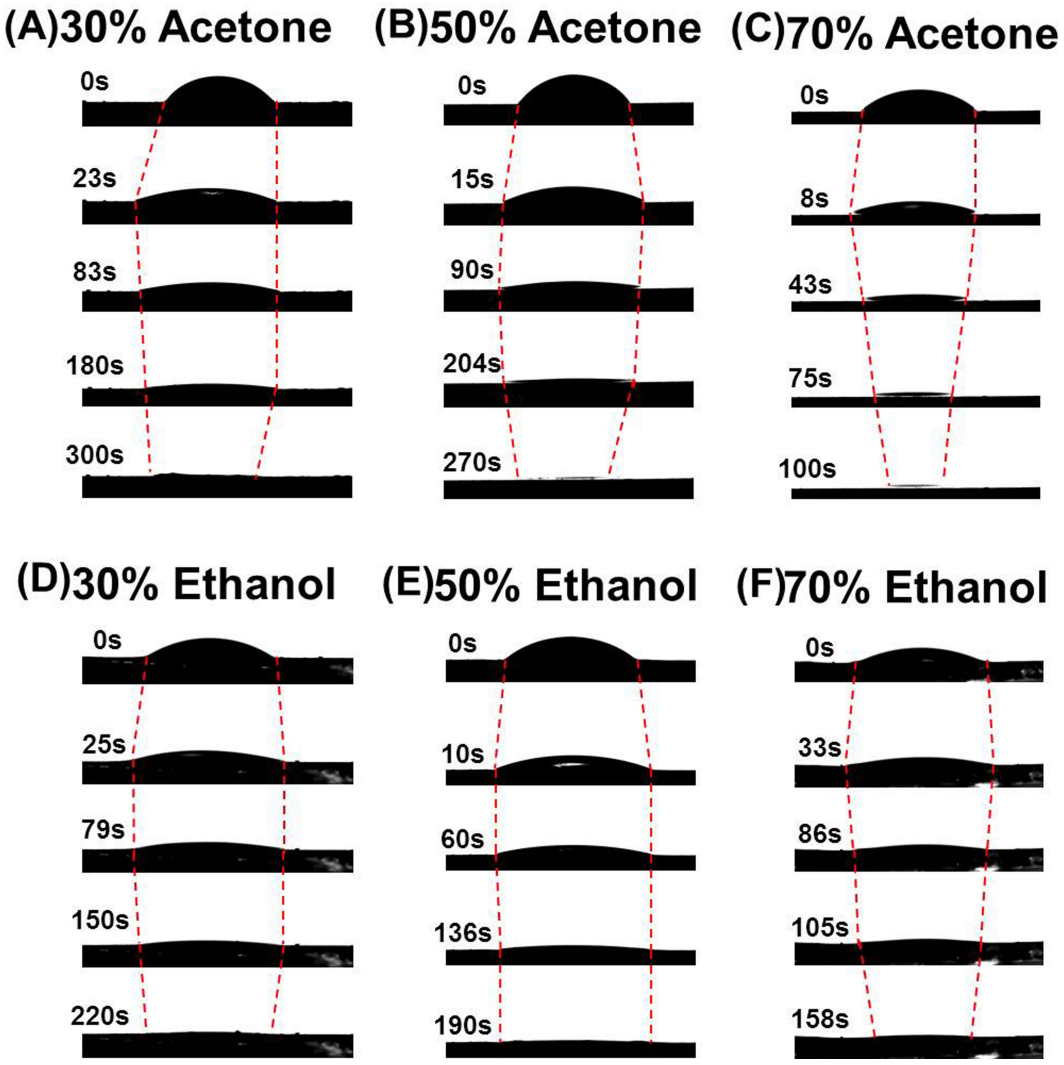

Figure S4. The side-view morphology of droplets with varied acetone or ethanol concentration on PIL films during evaporation process.

Figure S3-S4 present the *in-situ* dewetting process of the various solvent upon the PIL film. The red dash line indicates the evolution of the three phase contact line of the droplets during evaporation.

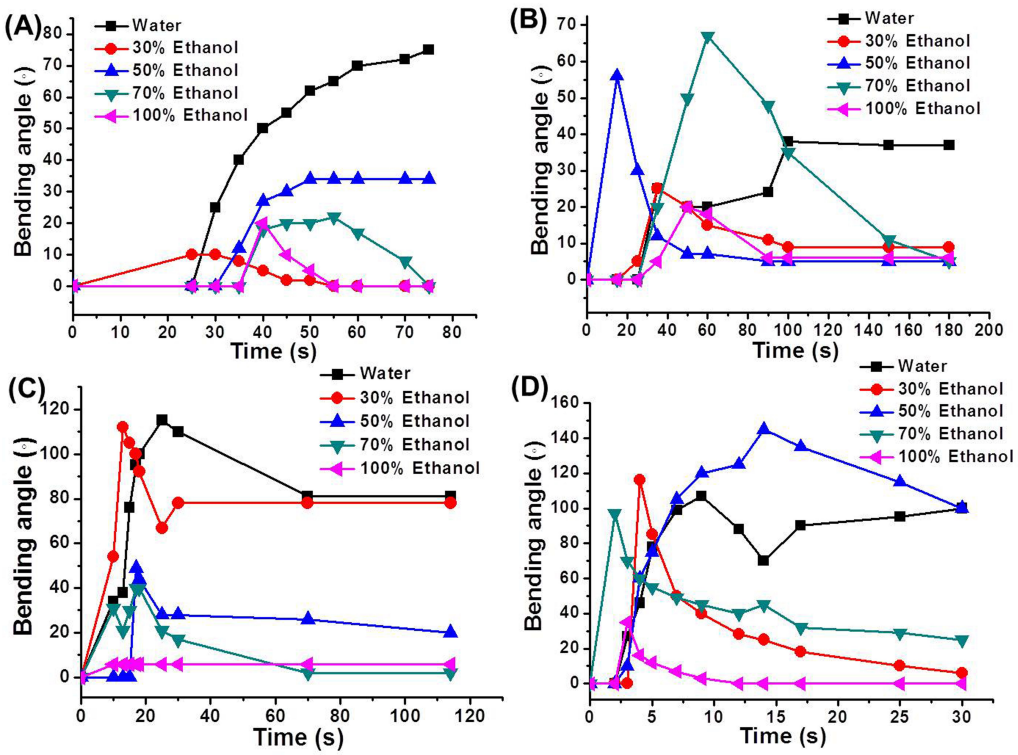

Figure S5. The response process (bending angle with time) of the actuations containing (A)25%, (B)50%, (C)75%, (D)100% PIL in various ethanol systems.

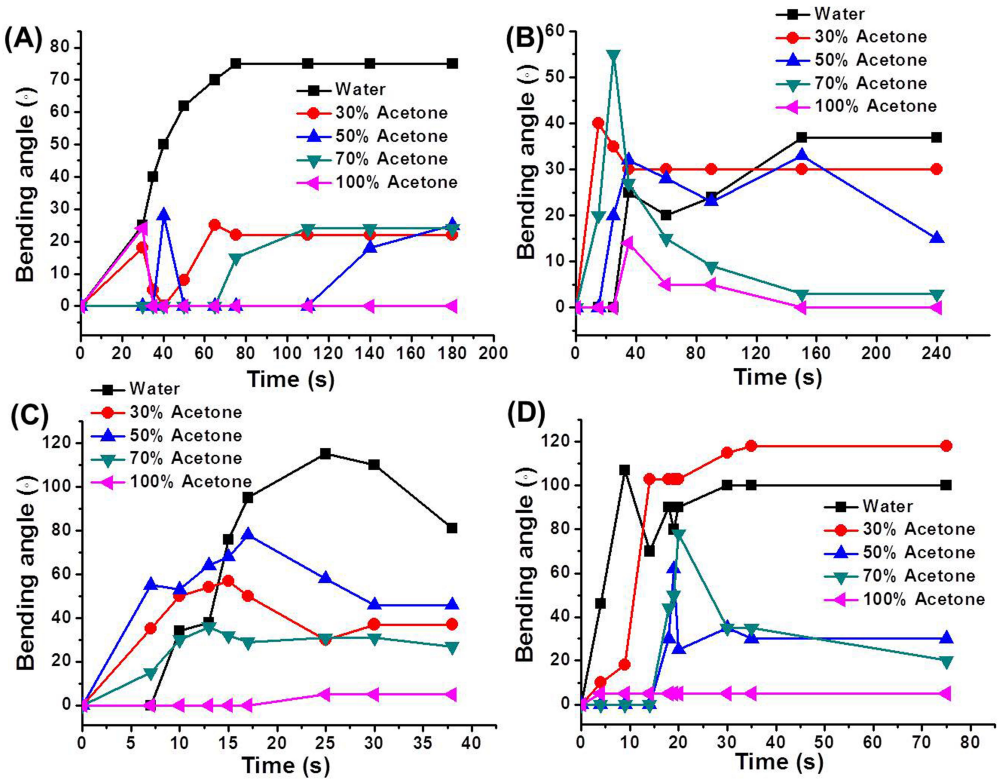

Figure S6. The response process (bending angle with time) of the actuations containing (A)25%, (B)50%, (C)75%, (D)100% PIL in various acetone systems.

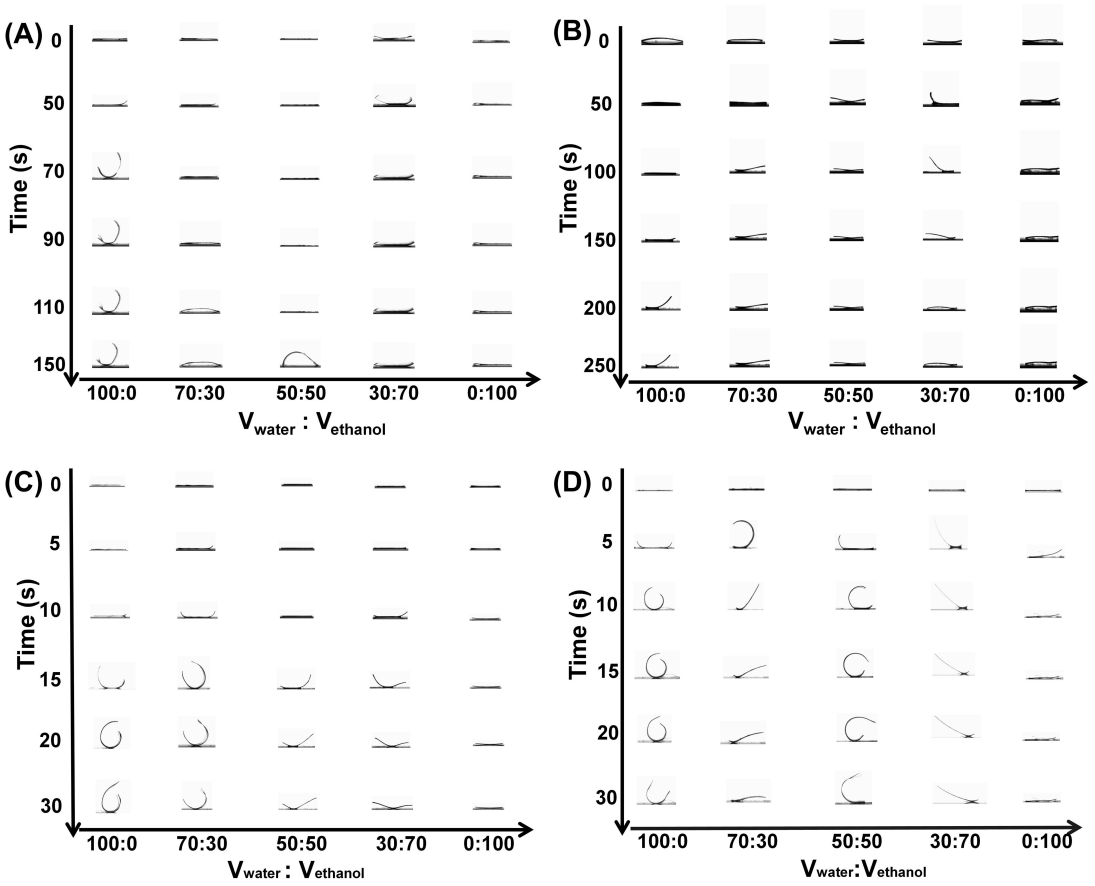

Figure S7. Optical photographs of the actuations during the response process in various ethanol systems. PIL content: (A) 25%, (B) 50%, (C) 75%, (D) 100%.

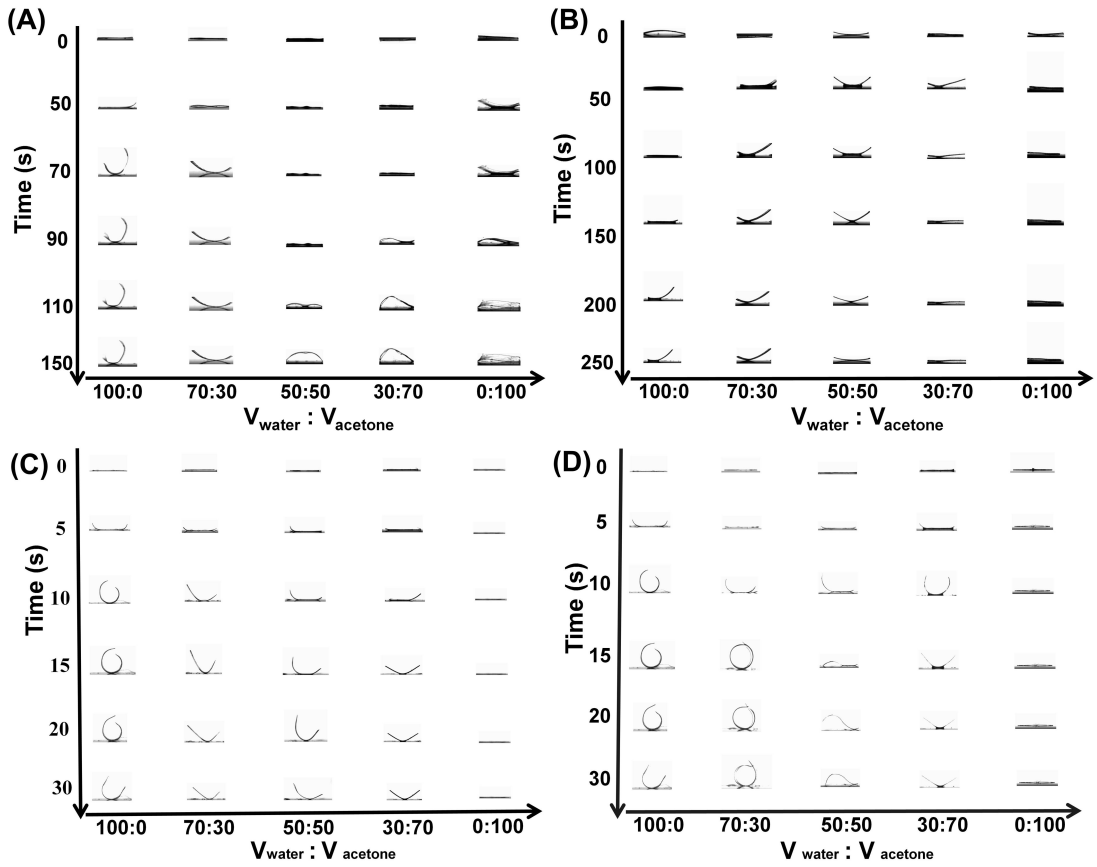

Figure S8. Optical photographs of the actuations during the response process in various acetone systems. PIL content: (A) 25%, (B) 50%, (C) 75%, (D) 100%.

Figure S5 and Figure S6 presents the evolutions of the bending angle for the actuations that containing various PIL in various solvent systems. **Figure S7** and **Figure S8** are the corresponding optical photographs of the samples during the actuating evolutions.

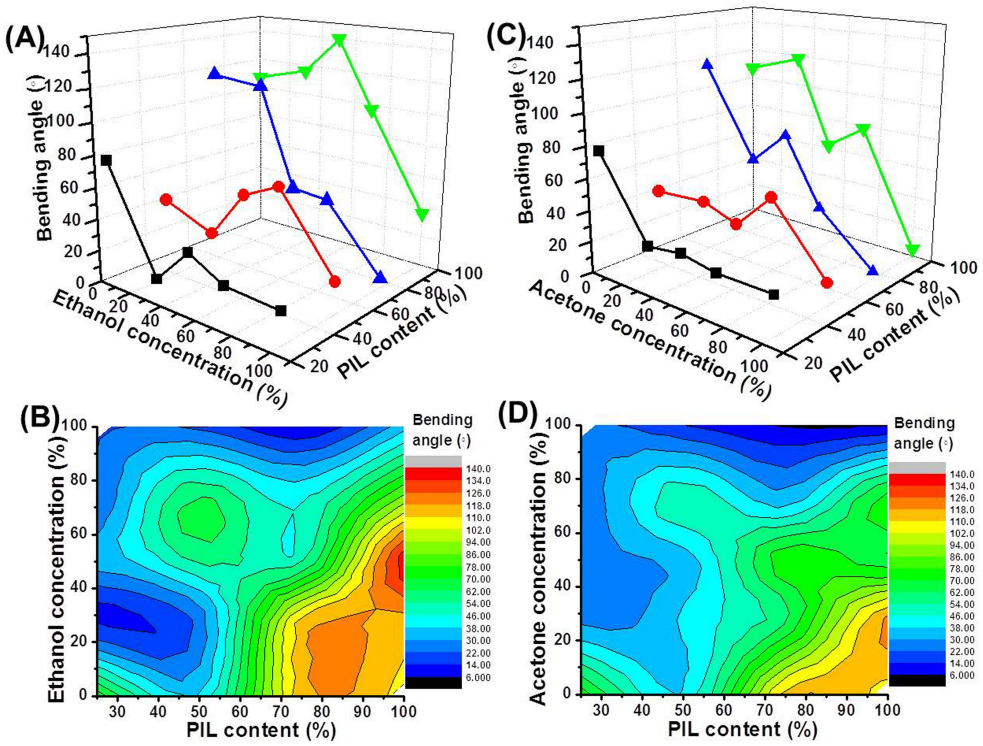

Figure S9. (A,B) Largest bending angle for the actuators at various ethanol systems. (C,D) Largest bending angle for the actuators at various acetone systems.

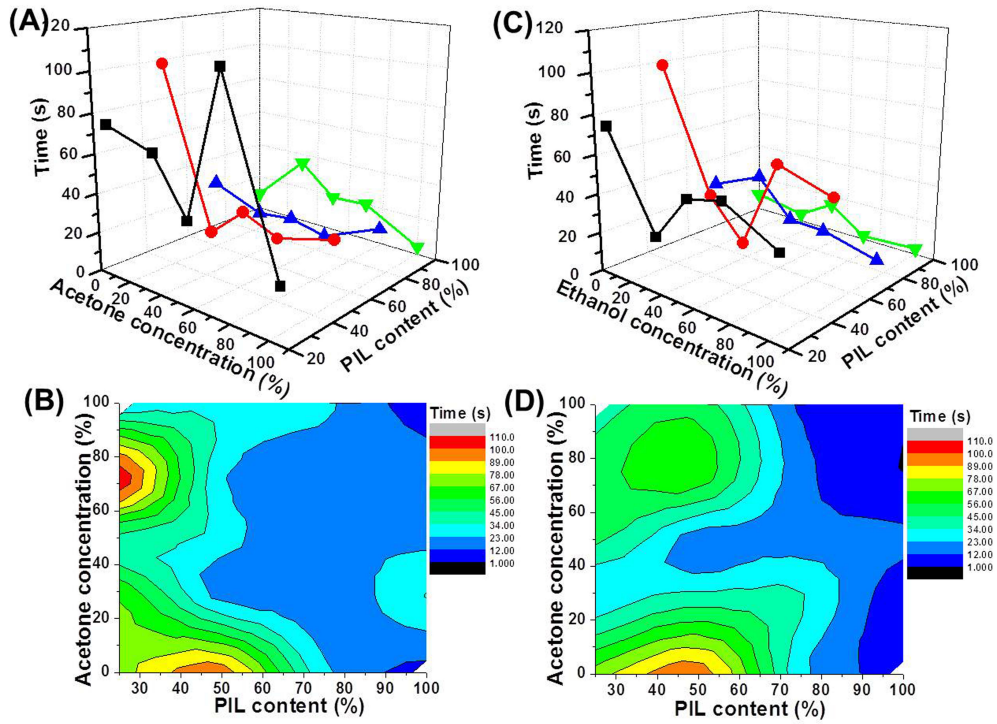

Figure S10. (A,B) Response time for the actuators achieving largest bending angle at various acetone systems. (C,D) Response time for the actuators achieving largest bending angle at various ethanol systems.

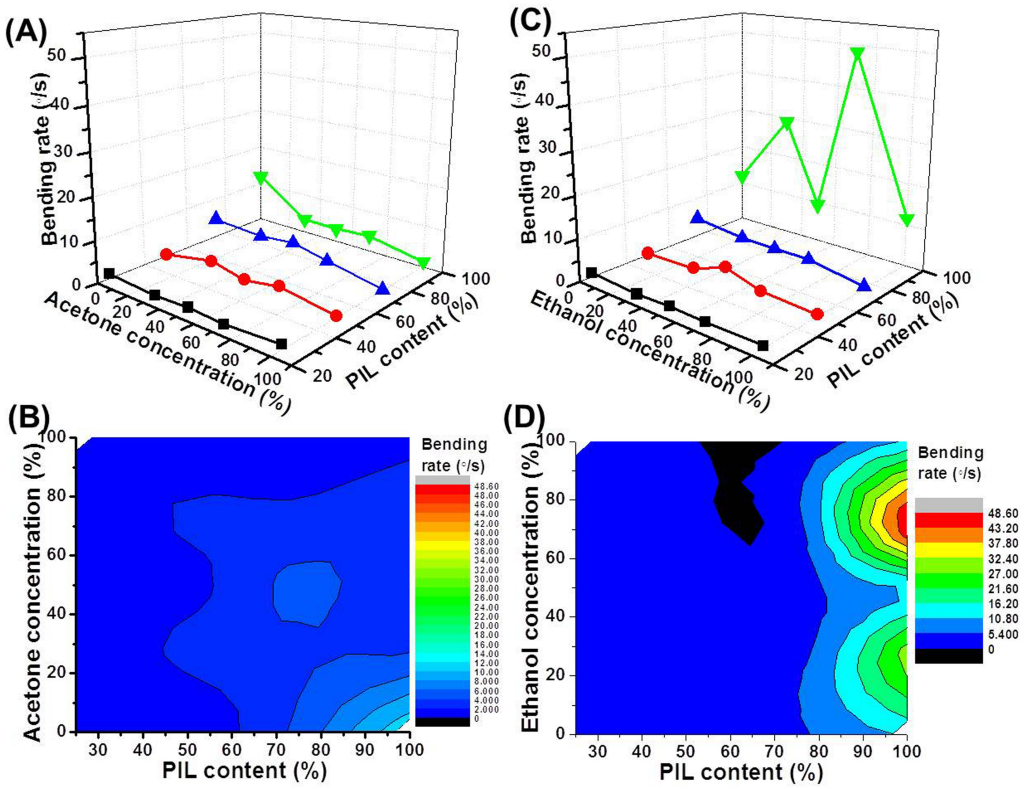

Figure S11. (A,B) Response rate for the actuators at various acetone systems. (C,D) Response rate for the actuators at various ethanol systems.

Figure S9-S11 show the largest bending angle, response time and response rate for the actuators at various solvent systems, respectively.

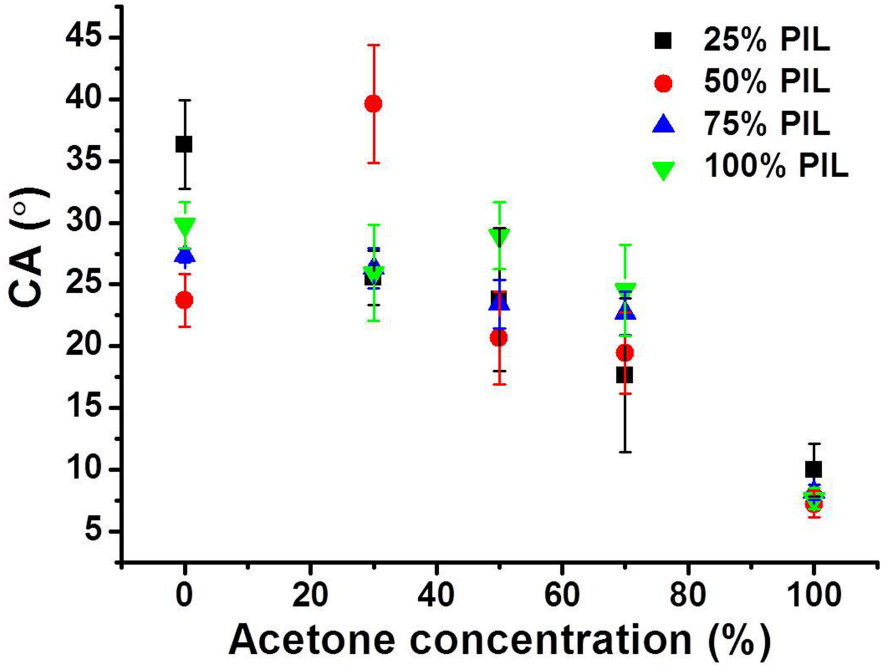

Figure S12. The contact angle (CA) of the droplet with various acetone/water mixing ratio on the surfaces with various PIL content.

Because acetone droplet is easier to wetting the PIL surface than the water droplet, the contact angle (CA) gradually decreases with increasing the acetone concentration on the surfaces with various PIL content. The smaller CA could bring about stronger interactions between the solvent molecular and the PIL polymer chain.

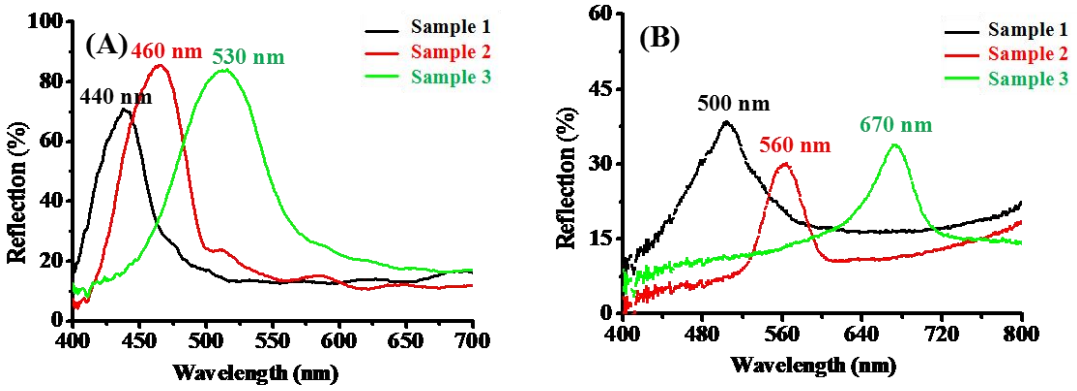

Figure S13. UV-vis spectra for the sample before (A) and after (B) being immersed into the acetone. It was found that the stopband of the samples (A) is 440, 460, 530 nm respectively, and the stopband of the sample red-shifted to 500, 560, 670 nm respectively. The spectra intensity lowers and the spectra turns to non-symmetric after swollen process. These phenomenon could be attributed to the degraded structure arousing from the solvent swollen. Otherwise, the red-shift of the spectra signal indicates the swelling of the sample, which can be used for the monitor of the swelling process for the sample.